

Measurements of CO₂ in a multipass cell and in a hollow-core photonic bandgap fiber at 2 μm

J.A. Nwaboh · J. Hald · J.K. Lyngsø · J.C. Petersen · O. Werhahn

Received: 1 February 2012 / Revised version: 29 March 2012 / Published online: 26 May 2012
© Springer-Verlag 2012

Abstract Recently, hollow-core photonic bandgap fibers (HC-PBFs) for use in the 2 μm wavelength region have become available. We have employed tunable diode laser absorption spectroscopy (TDLAS) to quantify CO₂ in nitrogen, injected into a HC-PBF. Our spectrometer contains both an HC-PBF-based absorption cell and an astigmatic Herriott multipass gas cell. The Herriott cell was used for comparison with the HC-PBF cell. The HC-PBF cell's sensitivity and limit of detection were calculated to be $3.5 \times 10^{-4} \text{ cm}^{-1} \cdot \text{Hz}^{-1/2}$ and 59 ppm·m, respectively. To substantiate the spectrometer performance, a measurement was done in the Herriott cell probing a reference gas mixture with nominal 400 μmol/mol CO₂ in N₂. The spectrometric results were in good agreement with the reference value. The relative standard uncertainty of the spectrometric result was found to be at the ±2 % level.

1 Introduction

In the past decades, advances in laser technology and spectroscopic methods have led to improvements in the measurement sensitivity and the accuracy of the spectroscopic determination of trace gas concentrations. The monitoring of the CO₂ molecule is important in many fields of science, which is manifested by the numerous papers addressing this issue [1–13]. The CO₂ molecule can be monitored at many wavelengths. With the availability of 2 μm lasers, monitoring CO₂ in this wavelength region becomes attractive due to its strong absorption bands, while still relying on near infrared optics.

In order to achieve high sensitivity and improved signal-to-noise ratios, multipass gas cells such as the Herriott cell [14] have been used to perform spectrometric measurements [15, 16]. Detection limits in the nmol/mol have been reached [17]. However, because of the typically large size and volume of multipass cells, they are rarely used for in situ measurements. For this purpose, compact (or even hand held) spectrometers are desirable.

HC-PBFs have been reported to be promising for the development of compact spectrometers, suitable for, e.g., environmental measurements and exhaled breath gas analysis [18–20]. HC-PBFs have the advantage that the absorption length can be chosen to be very long (several meters) while a compact design can be maintained where the fiber is coiled up. However, they have a frequency dependent transmission, which has to be taken into account when extracting quantitative data [18]. One major drawback when using HC-PBFs in gas sensors is the long gas filling time of the fiber [21, 22]. The filling time can be shortened in principle by drilling radial holes in the fiber or simply by using multiple short sections of fiber [18], but this is likely to influence the fiber transmission properties. The fact that the

J.A. Nwaboh (✉) · O. Werhahn
Physikalisch-Technische Bundesanstalt, Bundesallee 100, 38116
Braunschweig, Germany
e-mail: javis.nwaboh@ptb.de
Fax: +49-531-592693123

J. Hald · J.C. Petersen
Danish Fundamental Metrology, Matematiktorvet 307, 2800
Kongens Lyngby, Denmark

J. Hald
e-mail: jha@dfm.dtu.dk

J.K. Lyngsø
NKT Photonics A/S, Blokken 84, 3460 Birkerød, Denmark
e-mail: jkl@nktphotonics.com

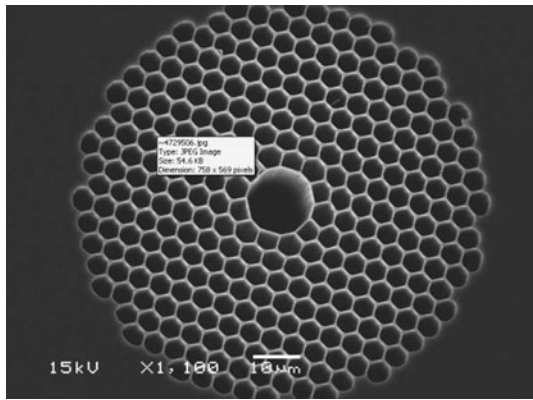


Fig. 1 Cross section of the hollow core photonic band gap fiber (HC-PBF) used provided by NKT Photonics. The central hollow core is used as the absorption gas cell, which is filled and pumped from both ends

fiber lengths can be tailored to any desirable length means that HC-PBF gas cells offer matched path lengths to any application without relying on multiples of any fixed physical length footprint.

Measurements of gas concentrations using HC-PBFs have been reported by several groups [21–23], but HC-PBFs for the 2 μm region, where CO_2 has strong absorption bands, have only recently been developed. In this work we report, to our knowledge, the first measurements of CO_2 amount fractions using a HC-PBF designed for a transmission window around 2 μm . Figure 1 shows a cross section of the HC-PBF structure used. Contrary to reports dealing with pure gases, we measured a gas mixture derived by first injecting CO_2 into the fiber and subsequently adding nitrogen as the matrix gas. This was to monitor the filling time of the HC-PBF due to the addition of N_2 compared to previous studies [12] where only a single molecular species was filled into the fiber.

We validated the performance of the HC-PBF with simultaneous measurements performed in an astigmatic Herriott multipass gas cell under the same experimental conditions. A further measurement, performed on a reference gas mixture, using only the Herriott cell was used to confirm the spectrometer's performance. The suitability of determining the amount-of-substance fraction was also demonstrated in that way.

2 Theory, conceptual background

An absorption spectrum can be quantitatively related to the amount-of-substance fraction of a gas species using the Beer–Lambert law. The Beer–Lambert law states the relationship between the incident radiation Φ_0 and the trans-

mitted radiant power Φ through a homogenous absorbing medium of thickness z as

$$\Phi(\tilde{\nu}, z) = \Phi_0(\tilde{\nu}) \cdot \exp\{-\alpha(\tilde{\nu}) \cdot z\} \quad (1)$$

where the quantity $\alpha(\tilde{\nu})$ is the absorption coefficient at frequency $\tilde{\nu}$. The absorption coefficient is proportional to the density of the absorbing medium n and is expressed as

$$\alpha(\tilde{\nu}) = \sigma(\tilde{\nu}) \cdot n = S_T \cdot r_{\text{iso}} \cdot g(\tilde{\nu} - \tilde{\nu}_0) \cdot n \quad (2)$$

The absorption cross section $\sigma(\tilde{\nu})$ depends on the normalized line profile function $g(\tilde{\nu} - \tilde{\nu}_0)$ centered at $\tilde{\nu}_0$ and the line strength S_T of the molecular transition at gas temperature T . The latter is reported for a certain abundance of the probed isotope and in cases needs to be corrected for the actual present isotopic abundance by means of r_{iso} . When probing a $^{12}\text{C}^{16}\text{O}_2$ excitation we have $r_{\text{iso}} = x_{12\text{C}^{16}\text{O}_2} / x_{12\text{C}^{16}\text{O}_2\text{HIT}}$, where $x_{12\text{C}^{16}\text{O}_2}$ and $x_{12\text{C}^{16}\text{O}_2\text{HIT}}$ are the abundance of $^{12}\text{C}^{16}\text{O}_2$ in the sample and the conventional value set by HITRAN [24], respectively.

Relying on the ideal gas law, the molecular density n of the absorbing species can be expressed in terms of the partial pressure p_{partial} of the absorbing molecule and the gas temperature. The partial pressure can be related to the total pressure p_{total} using the amount-of-substance fraction of the absorbing species, $x_{\text{species}} = p_{\text{partial}} / p_{\text{total}}$. Introducing the spectral absorbance $A(\tilde{\nu}) = -\ln(\Phi(\tilde{\nu}, L) / \Phi_0(\tilde{\nu}))$, as well as the total path length L , and making use of the normalization of $g(\tilde{\nu} - \tilde{\nu}_0)$, Eqs. (1) and (2) can be combined to an integral form

$$\begin{aligned} x_{\text{species}} &= \frac{k_B \cdot T}{L \cdot p_{\text{total}} \cdot S_T \cdot r_{\text{iso}}} \int_{-\infty}^{\infty} A(\tilde{\nu}) d\tilde{\nu} \\ &= \frac{k_B \cdot T}{L \cdot p_{\text{total}} \cdot S_T \cdot r_{\text{iso}}} \cdot A_{\text{line}} \end{aligned} \quad (3)$$

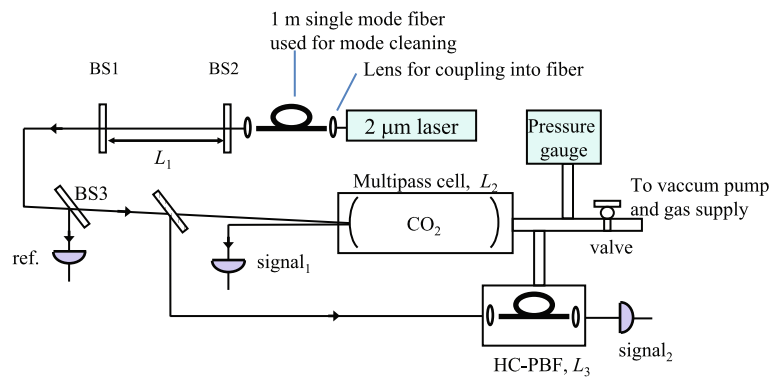
where A_{line} is the line area.

For spectroscopic measurements using HC-PBFs the filling time is an important parameter. The filling time has been investigated for pure gases in the high and low pressure regime in a previous study [22], where the time for filling an empty HC-PBF to 99.4 % of the final gas content is given for a pure gas in the low pressure regime by

$$\tau = \frac{3L^2}{2d} \sqrt{\frac{\pi m}{8kT}} \quad (4)$$

Here, d is the inner diameter of the HC-PBF, m is the molecular mass and T is the temperature. The boundary between the low pressure and high pressure regimes is defined in [22] as the regime with a Knudsen number $Kn = \lambda/d$ equal to one, where λ is the mean free path between intermolecular collisions and d is the HC-PBF core diameter. For CO_2 in a 15 μm fiber, the Knudsen number equals one at a pressure of about 6 hPa. In the high pressure regime, the filling is somewhat faster [22], so Eq. (4) can be used as an upper limit. If a mixture of different gases is used, the filling time will

Fig. 2 Schematic diagram of the setup used for CO₂ quantification. *BS1* and *BS2* are partially reflecting mirrors on flip mounts, which constitute an interferometer. *BS3* is used as beamsplitter. *L*₁, *L*₂, and *L*₃ are the lengths of the interferometer, the Herriott cell and the HC-PBF. Optical power is detected at ref., signal₁, and signal₂



be influenced by differences in the diffusion constants of the individual gas components. Due to the molecular selectivity, spectroscopic sensing inside the fiber core enables monitoring of fiber length averaged amount-of-substance fractions for individual species, which may be used to analyze the diffusion of various species into a hollow-core fiber. To this end, the following experimental work has been started.

3 Experimental

Figure 2 shows a schematic of the setup used for the CO₂ measurements. A commercial continuous wave (cw), thermoelectrically cooled, distributed-feedback (DFB) tunable diode laser (TDL) emitting radiation at 2 μm (nanoplus 2004 nm) was used to probe the R(12) line of CO₂ at 4987.31 cm⁻¹ (2005.09 nm).

The laser temperature tunability of 0.26 nm/°C was used to tune the emission wavelength. In order to perform spectrometric measurements, the wavelength of the DFB diode laser was swept with a current ramp at a frequency of 5 Hz. After collimation, the TDL beam with an elliptical profile passed through a 3 m single mode fiber (Thorlabs SM2000) with angled connectors used for mode cleaning in order to get the best possible coupling of light into the HC-PBF. The optical power from the DFB laser was about 2 mW, and the transmission through the mode cleaning fiber was 15%. From the SM2000 specifications, we derive a theoretical M^2 value of about 1.05 for the beam after the mode cleaning fiber [25]. A number of lenses (not shown) were used to optimize the coupling into the Herriott cell and the HC-PBF. An interferometer based on partially reflecting mirrors on flip mounts was used to establish the frequency axis before and after spectroscopic measurements. A beamsplitter divided the beam into a reference, going to a reference detector (ref.), and a sample beam. The sample beam could be directed to either the Herriott multipass cell or the HC-PBF-based cell. The output from either cell was sampled on a photo detector (New Focus 2034). The astigmatic Herriott cell (Aerodyne AMAC-36) was aligned to a measured path

length of $L_2 = (41.88 \pm 0.02)$ m, realized on a footprint of a 20 cm mirror-separated base path. A simple laser distance meter was used to measure the cell's optical path length.

The HC-PBF (HC-2000-01) was manufactured by NKT Photonics [26], its geometrical length was $L_3 = (5.27 \pm 0.01)$ m and the core diameter is specified to $d = 15$ μm. The HC-PBF was enclosed in a sealed box, which was directly connected to the same vacuum line as the Herriott cell as shown in Fig. 2. We typically obtained coupling efficiencies of the laser light into the HC-PBF cell of about 15%, which is smaller than the 65%–85% coupling efficiencies for HC-PBFs in the 1.55 μm range using identical setups [12, 22]. The fiber design should allow similar coupling efficiencies as in the 1.55 μm range. However, it was not possible for us to improve the coupling into the HC-PBF despite attempts to optimize the spatial mode matching and recleaning the HC-PBF. A similar coupling efficiency was found for a 21 m piece of the same type of HC-PBF. Coupling efficiencies were measured by means of the quotient of transmitted and incident light power for different fiber lengths, such that the attenuation of the fiber, specified to be 20 dB/km by the manufacturer, was included, as well as the fixed prealignment of the fiber with respect to the in and out coupling lenses inside the sealed box.

The signals from the two photo diodes (the reference and the sample signals) were digitized by a Tektronix DPO 3034 oscilloscope at a sampling rate of 5 MS/s.

For spectroscopic measurements the 41.88 m Herriott cell and the HC-PBF were first evacuated and then filled with the gases. The system was kept untouched for some time to enable the gases to diffuse into the HC-PBF from the fiber ends.

Figure 3 shows typical transmission data for the HC-PBF cell and the Herriott cell when the R(12) line and four neighboring lines were probed in pure CO₂ kept at a pressure of 25 hPa.

Figure 4 (left) shows the interference fringes from the simple interferometer measured with the reference detector. These fringes are used to generate the frequency axis. The distance between the two mirrors (BS1 and BS2) in the interferometer is measured with a laser distance meter to be

(318.1 ± 1.5) mm, which gives a frequency difference of 471 MHz between zero crossings in Fig. 4 (left). The fringe amplitude decreases during the scan because the scan ramp applied to the laser drive current affects both laser power and laser frequency. This coupling between laser frequency and output power is not visible in the spectra in Fig. 3 due to the normalization of the signal detector output with the reference detector output.

Figure 4 (right) shows a comparison of the experimental position of 4 CO₂ absorption lines within the tuning range of the laser (see Fig. 3) with those of the HITRAN [24] database. A linear function is fitted to the data in Fig. 4 (right), and the slope of 0.989 ± 0.003 shows consistency between the interferometer data and the HITRAN [24] peak positions. The overall standard uncertainty of the frequency scale is about 1 %.

4 Results and discussions

A gas mixture of CO₂ in nitrogen was used for studying the performance of the HC-PBF setup. The gas mixture was prepared by the injection of 5 hPa of CO₂ into the evacuated vacuum system (the Herriott cell plus the HC-PBF)

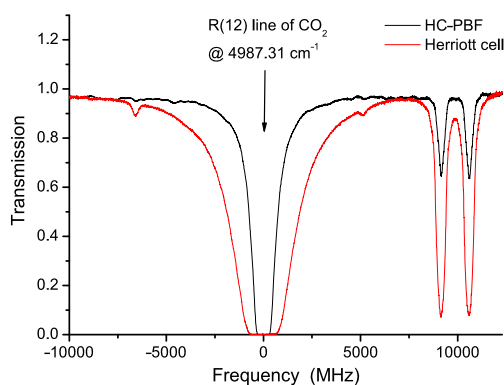
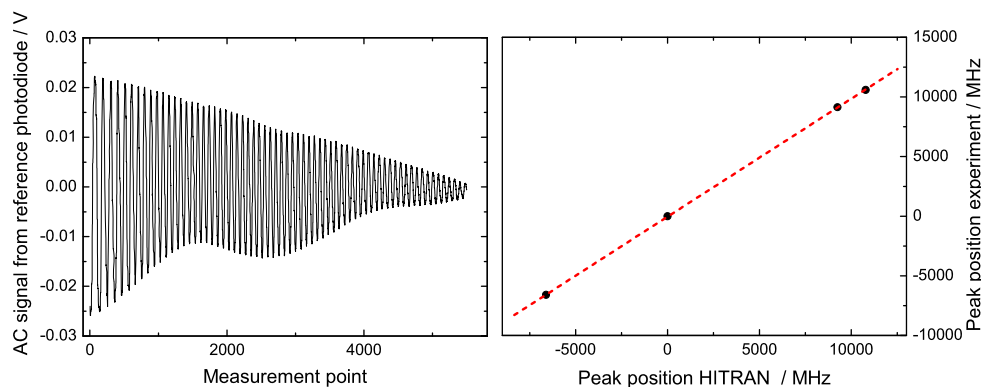


Fig. 3 Transmission data from the astigmatic Herriott cell (red) and the HC-PBF cell (black) as a function of frequency. Both cells are filled with pure CO₂ at a pressure of 25 hPa. Note that their path lengths differ by approximately a factor of 8

Fig. 4 Signal from the interferometer used for frequency calibration. The frequency difference between zero crossings is 471 MHz (left). Comparison of the experimental peak positions of 4 absorption lines with those of the HITRAN database showing consistency with the measured interferometer length (right)



and the subsequent addition of nitrogen and reduction of total pressure to achieve a CO₂ amount fraction of about 1300 μmol/mol at a total pressure of about 150 hPa. We monitored the time necessary to attain equilibrium, i.e., a measured amount fraction of 1300 μmol/mol, with the HC-PBF spectrometer by repeated data collection. To this end, a period of more than 3 days was necessary as detailed in the following. For each data set, we first compared the HC-PBF line area results with those derived from the Herriott cell signals. Figure 5 shows transmission data as a function of laser detuning measured at day one after the gases were fed into the system. The scan time of an individual spectrum was set to 18 ms which transferred to spectral window of 30 GHz as shown in Fig. 6. Only single scans were considered for analysis, i.e., no averaging, in the present study.

The measured transmission data in Fig. 5 were fitted to the expressions in Eqs. (1) and (2), where a Voigt profile was used as the normalized line profile function $g(\tilde{\nu} - \tilde{\nu}_0)$. The fit provided the value for the line area. The noise in the residuals from the fit to the HC-PBF data shows that the frequency dependent transmission of the HC-PBF is compa-

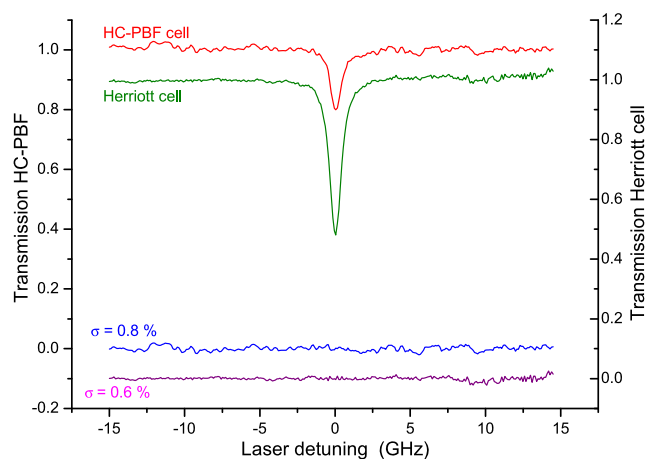


Fig. 5 Transmission data of the Herriott cell and the HC-PBF as a function of laser detuning recorded one day after filling the system with CO₂ and N₂. The blue and purple graphs are the residuals of the least squares fits to the transmission data. Total pressure was 154 hPa

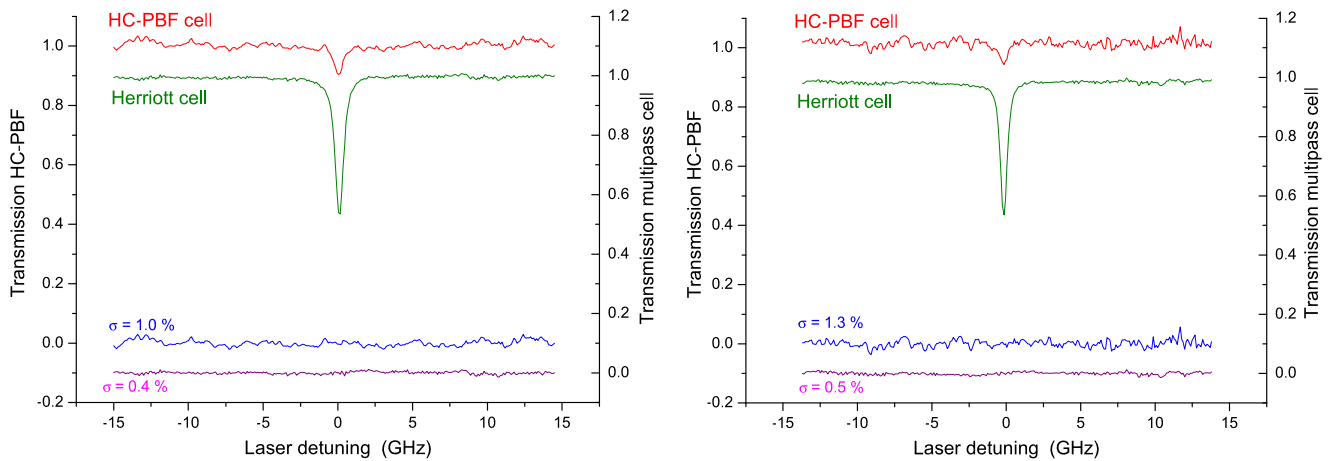


Fig. 6 Transmission of the HC-PBF cell and the Herriott cell as a function of laser detuning measured at day two and a total pressure of 105 hPa (left), and at day three and a total pressure of 78 hPa (right)

Table 1 Derived line areas from Herriott cell data and HC-PBF with respect to total gas pressure, ratios between individual data and respective variations

Day #	Total pressure /hPa	Line area/MHz		Line area ratio between cells	Variation factor to 1st day	
		Herriott cell	HC-PBF		Pressure	HC-PBF Line area
1	154	838 ± 11	279 ± 7	3	–	–
2	105	516 ± 7	119 ± 7	4.3	1.5	2.3
3	78	406 ± 6	60 ± 7	6.8	2.0	4.7

able to similar measurements on HC-PBFs in the telecom range at 1550 nm [18]. The flat structure of the residuals apparently differs from the oscillatory structures reported in [18], but this is essentially due to the much larger scan range used in the present work. The standard deviation σ of the residuals for the HC-PBF data and the Herriott cell data were found to be 0.8 % and 0.6 %, respectively.

As mentioned above, we observed that the signal remained unstable even a day after the gas filling. Figure 6 shows data measured at day two and day three. We reduced the total pressure from the initial 154 hPa to 105 hPa right after the measurements on day one, and we reduced the pressure further down to 78 hPa after the measurements on day two. The pressure was reduced to check for changes in the signal-to-noise ratio after each day. The residuals of the fit to the HC-PBF data in Fig. 6 are slightly noisier than those in Fig. 5. This is within the typical variations in the frequency dependent HC-PBF transmission due to small changes in the HC-PBF coupling [18].

Comparing the spectral features in the HC-PBF data, i.e., in Figs. 5 and 6, there is an obvious decrease of the signal-to-noise ratio. However, this is not completely attributable to the reduction of the total pressure from day one to day three. This is evidenced by the ratio of pressures compared to those of the line areas for the three data sets in Table. 1. Whereas the pressure was just decreased by a factor of less than 2, the

line area decrease from day one to day three results in a factor of nearly 5. This indicates that the CO₂, which was filled into the system before the nitrogen, was further trapped inside the fiber when N₂ was added. The filling time for a pure gas calculates with Eq. (4) to be about 2 hours. However, the added N₂ apparently increased the diffusion time for the CO₂ coming out of the fiber to be replaced by nitrogen to a final inside equilibrium mixing ratio.

This is also confirmed by the fitted line areas obtained from the simultaneously measured Herriott cell data compared to the HC-PBF results, which are summarized in Table 1. A fitted line area of (838 ± 11) MHz for the Herriott cell data at day one has to be compared to the line area measured in the HC-PBF cell computed to be (279 ± 7) MHz for the data presented in Fig. 5. The ratio between these two line areas is 3.0. The line area for the Herriott cell data at day two is (516 ± 7) MHz and that of the HC-PBF cell data is (119 ± 7) MHz. At day three, the line areas for the Herriott cell and HC-PBF data were derived to be (406 ± 6) MHz and (60 ± 7) MHz, respectively. As shown in Table 1, the ratio from the two signals was developing from 3.0 at day one, and 4.3 at day two (Fig. 6 left), to 6.8 at day 3 (Fig. 6 right). The expected ratio, however, resulting from the path lengths of the two cells reads 7.9 instead. The discrepancy is attributed to a much longer time constant for the gas exchange inside the HC-PBF compared to the pure filling with gas starting at vacuum which was described by Eq. (4). The

mixing of the two gas species inside the HC-PBF apparently takes place on a much longer time scale.

It should be noted here that, of course, we are not able to derive any quantitative analysis from the observations presented here. However, choosing this procedure we were pointing on principle options to study diffusion processes by means of such fiber setups. Pressure gradients inside and outside the HC-PBF were not that large, such that the long lasting struggle of CO₂ molecules exchanging their positions with nitrogen molecules to reach equilibrium gas mixing conditions also inside the fiber could not have been expected a priori. Typical situations encountered in gas monitoring would comprise premixed gases, where total gas exchange time constants of the HC-PBF are more in focus than diffusion rates of individual gas constituents. Nevertheless, individual diffusion rates may have to be taken into account in gas sensing applications using long HC-PBFs.

For the HC-PBF setup, we calculated a sensitivity figure according to [27],

$$S_y = \frac{s_\alpha}{\sqrt{1/\tau_{\text{scan}}}}$$

by means of the standard deviation s_α of the baseline absorption coefficient (see Eq. (1)) and the scan time τ_{scan} of 18 ms for the data in Fig. 6 (right) to be $3.5 \times 10^{-4} \text{ cm}^{-1} \cdot \text{Hz}^{-1/2}$. The detection limit scales inversely with the fiber length with a constant estimated to be 59 ppm·m for CO₂ at atmospheric pressure.

Comparing the line areas of the Herriott cell data measured at day one to that at day three yields a ratio of ~ 2 . This agrees with the pressure variation specified in Table 1, and shows that the spectral feature and, with that, the measurement result of the Herriott cell data remains much more stable across the different days and unchanged because of the faster mixing in the larger volume of the Herriott cell compared to the HC-PBF. This is very much in contrast to the large variation of line areas by a factor of 4.7 derived from HC-PBF data.

Figure 7 summarizes the ratios of the line areas of the Herriott cell data to those of the HC-PBF cell as a function of time. The ratio of the line areas approached the cell length ratio of 7.9 on the third day, indicating that it takes about 4 days to attain equilibrium. Apparently, slower gas and molecular dynamics may be involved when using the HC-PBF as an absorption gas cell than implicated by experimental results on pure substances reported in [22]. Even though in situ gas measurement applications would be in favor of measuring already premixed gas mixtures, gas exchange, and persisting gas mixture samples inside HC-PBFs may compromise the usability of the HC-PBF cell concept. Mixtures including species with large dipole moments like, e.g., ammonia, which tend to stick to the surface of the HC-PBF, can be expected to involve slow gas dynamics in HC-PBFs. Species-dependent diffusion is expected to have no

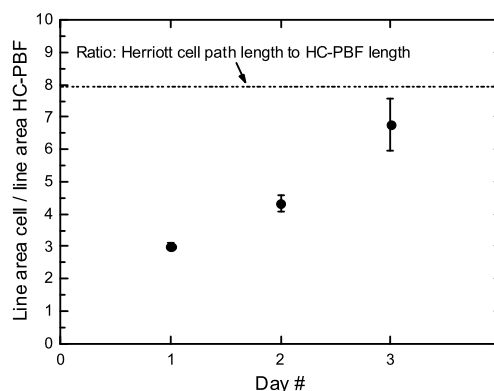


Fig. 7 Ratio of the measured line areas, Herriott cell to that of the HC-PBF cell. From the path lengths a ratio of 7.9 was expected (*dashed line*)

or small effect on the time required for reaching equilibrium for pre-mixed gasses.

The line area of the Herriott cell data corresponds to an amount fraction of 1350 $\mu\text{mol/mol}$ CO₂ calculated by means of Eq. (3). This is in the range of the expected value computed from the mixing of the initial partial pressures of CO₂ and N₂, although the uncertainty associated with the concentration derived from initial partial pressures is significantly larger than the uncertainty on the Herriott cell data.

In order to evaluate the performance of the spectrometric setup used for the simultaneous HC-PBF and Herriott cell measurements presented above, we performed a benchmark test on a Messer reference gas mixture certified to consist of 399.4 $\mu\text{mol/mol}$ CO₂ in N₂ with a relative standard uncertainty of $\pm 0.5\%$. This test involved a separate measurement in the Herriott cell on the reference gas mixture following the “Traceable Infrared Laser-Spectrometric Amount fraction Measurement” (TILSAM) protocol [28].

The results obtained are shown in Fig. 8, where the determined line area of the R(12) line is plotted as a function of the total pressure. The linear dependence predicted in Eq. (3) is evident, and a general least squares method [29] was applied to derive the spectroscopically determined amount fraction. The measured values of line area and pressure together with measured values for cell length and temperature were used as input to the analysis. For this analysis, the line strength figure of the probed R(12) line was taken from [12, 30]. Equation (3) was used as the constraint for the analysis, and the least squares analysis gave a measured amount fraction of 399.6 $\mu\text{mol/mol}$ CO₂ with a relative standard uncertainty of $\pm 2\%$. Based on the good agreement in this performance test, the Herriott multipass gas cell data provide a reliable reference for the HC-PBF’s measurements discussed above.

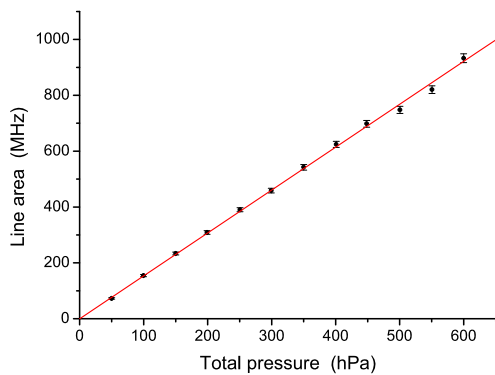


Fig. 8 The figure shows a plot of the determined line area of the R(12) line of CO₂ at 4987.31 cm⁻¹ as a function of the total pressure for a (399.4 ± 2.0) μmol/mol reference gas. The *error bars* represent the estimated standard uncertainties on the individual data. The *solid line* represents the result from a general least squares analysis, from which the slope parameter yields the CO₂ amount fraction which was determined to be (399.6 ± 8.0) μmol/mol

5 Conclusions

The CO₂ molecule has strong absorption bands in the 2 μm wavelength region, thus making this wavelength region suitable for monitoring traces of CO₂. Working in the NIR has the advantage of lower costs due to established production lines of DFB diode lasers combined with the high technological level of optics and detectors. Relying on these issues might be beneficial to the development of compact CO₂ spectrometers for industrial applications. It is important that compact sensors for in situ measurements are developed and that measurement methods used by them are quantitative.

It has been shown that a HC-PBF transmitting at 2 μm can be used as a gas cell in a laser spectrometer setup allowing for a compact CO₂ monitoring system. The fiber transmission's frequency dependence, which sets a baseline in the spectroscopic signal, is comparable to the frequency dependence of fibers used in the telecom wavelength range at around 1550 nm. The applied filling process illustrates that very long equilibrium time may be observed when using HC-PBFs in gas sensing. Shorter time scales are expected when carefully prepared premixed gas samples are used. Furthermore, drilling radial holes in the fiber, which is the focus of future work, would increase accessible gas exchange rates and lead to a much shorter time scale to reach equilibrium conditions for the measurement process.

The proof-of-principle experiment demonstrated by our setup shall be viewed as a first step toward future applicability studies with HC-PBF-based sensors. The spectrometer performance benchmarked by means of Herriott cell-based CO₂ quantification showed excellent agreement with the specified amount fraction of a reference gas mixture.

Acknowledgements This work was partly performed within a EURAMET joint research project and received funding from the European

Union Framework Programme, ERA-NET Plus, under the iMERA-Plus Project—Grant Agreement No. 217257 and the European Metrology Research Programme which is jointly funded by the EMRP participating countries within EURAMET and the European Union. J.A.N. acknowledges the continued support from the Braunschweig International Graduate School of Metrology and the Institute of Physical and Theoretical Chemistry at TU-Braunschweig.

References

1. G. Castrillo, G. Gagliardi, G. Casa, L. Gianfrani, *Phys. Rev. A* **67**, 0625031 (2003)
2. J.A. Nwaboh, T. Desbois, D. Romanini, D. Schiel, O. Werhahn, *Int. J. Spectros.* (2011). doi:[10.1155/2011/568913](https://doi.org/10.1155/2011/568913)
3. I. Pouchet, V. Zéninari, B. Parvitte, G. Durry, *J. Quant. Spectrosc. Radiat. Transf.* **83**, 619 (2004)
4. T. Le Barbu, B. Parvitte, V. Zeninari, I. Vinogradov, O. Korablev, G. Durry, *Appl. Phys. B* **82**, 133 (2006)
5. M.R. McCurdy, Y.A. Bakhirkin, G. Wysocki, F.K. Tittel, *J. Biomed. Opt.* **12**, 1 (2007)
6. R.M. Mihalcea, M.E. Webber, D.S. Baer, R.K. Hanson, G.S. Feller, W.B. Chapman, *Appl. Phys. B* **67**, 283 (1998)
7. A. Castrillo, E. De Tommasi, L. Gianfrani, *Opt. Lett.* **31**, 3040 (2006)
8. V. Weldon, J. O'Gorman, P. Phelan, J. Hegarty, T. Tanbun-Ek, *Sens. Actuators B, Chem.* **29**, 101 (1995)
9. V. Ebert, S. Wagner, K. Wunderle, in *2nd International Workshop on Stable Isotope Ratio Infrared Spectrometry*, Florence, Italy (2007)
10. C. Corsi, F. D'Amato, M. De Rosa, G. Modugno, *Appl. Phys. B* **70**, 879 (2000)
11. M.M.J.W. Van Herpen, A.K.Y. Ngai, S.E. Bisson, J.H.P. Hackstein, E.J. Woltering, F.J.M. Harren, *Appl. Phys. B* **82**, 665 (2006)
12. G. Padilla Viquez, J. Koelliker Delgado, O. Werhahn, K. Jousten, D. Schiel, *IEEE Trans. Instrum. Meas.* **56**, 529 (2007)
13. D. Weidmann, G. Wysocki, C. Oppenheimer, F.K. Tittel, *Appl. Phys. B* **80**, 255 (2005)
14. D. Herriott, H. Kogelnik, R. Kompfner, *Appl. Opt.* **3**, 523 (1964)
15. C. Dyroff, P. Weibring, A. Fried, D. Richter, J.G. Walega, A. Zahn, W. Freude, P. Werle, *Appl. Phys. B* **88**, 117 (2007)
16. V. Ebert, J. Wolfrum, in *Optical Measurements-Techniques and Applications* (Springer, Berlin, 1994), pp. 273–312
17. L.K. Moskalenko, A.I. Nadezhdinskii, I.A. Adamovskaya, *Infrared Phys. Technol.* **37**, 181 (1996)
18. C.I. Falk, J. Hald, J.C. Petersen, J.K. Lyngsø, *Appl. Opt.* **49**, 3854 (2010)
19. A.M. Cubillas, J. Hald, J.C. Petersen, *Opt. Express* **16**, 3976 (2008)
20. J. Henningsen, J. Hald, J.C. Petersen, *Opt. Express* **13**, 10475 (2005)
21. Y.L. Hoo, W. Jin, C. Shi, H.L. Ho, D.N. Wang, S.C. Ruan, *Appl. Opt.* **42**, 3509 (2003)
22. J. Henningsen, J. Hald, *Appl. Opt.* **47**, 2790 (2008)
23. W. Jin, H.F. Xuan, H.L. Ho, *Meas. Sci. Technol.* **21**, 094014 (2010)
24. L.S. Rothman, I.E. Gordon, A. Barbe, D. Chris Benner, P.F. Bernath, M. Birk, V. Boudon, L.R. Brown, A. Campargue, J.-P. Champion, K. Chance, L.H. Coudert, V. Dana, V.M. Devi, S. Fally, J.-M. Flaud, R.R. Gamache, A. Goldman, D. Jacquemart, I. Kleiner, N. Lacome, W.J. Lafferty, J.-Y. Mandin, S.T. Massie, S.N. Mikhailenko, C.E. Miller, N. Moazzen-Ahmadi, O.V. Naumenko, A.V. Nikitin, J. Orphal, V.I. Perevalov, A. Perrin, A. Predoi-Cross, C.P. Rinsland, M. Rotger, M. Šimečková, M.A.H. Smith, K. Sung, S.A. Tashkun, J. Tennyson, R.A. Toth, A.C. Vandaele, J. Van-

- der Auwera, J. Quant. Spectrosc. Radiat. Transf. **110**, 533 (2009). HITRAN2008, <http://www.cfa.harvard.edu/HITRAN/>
25. P.A. Belanger, Opt. Eng. **32**, 2107 (1993)
26. NKT photonics (2012). Available at: <http://www.nktphotonics.com/>
27. B.E. Brumfield, J.T. Stewart, S.L.W. Weaver, M.D. Escarra, Sc.S. Howard, C.F. Gmachl, B.J. McCall, Rev. Sci. Instrum. **81**, 063102 (2010)
28. O. Werhahn, J.C. Petersen (eds.), *TILSAM* technical protocol V1_2010-09-29 (2010). http://www.euramet.org/fileadmin/docs/projects/934_METCHEM_Interim_Report.pdf
29. L. Nielsen, Metrologia **35**, 115 (1998). Erratum, Metrologia **37**, 183 (2000)
30. G. Wübbeler, G.J. Padilla Viquez, K. Jousten, O. Werhahn, C. Elster, J. Chem. Phys. **135**, 204304 (2011)